

Supplementary Materials: Systematic comparison of tsunami simulations at the Chilean coast based on different numerical approaches

Alternative mesh data

The following figure is complementary to the Figure 2 in the main text. In this figure, the resolution variations in the triangular mesh that have been adapted from the nested grids. As example, it depicts an area of Valparaíso including part of the grid 3 and grid 4 of the nested topo-bathymetry.

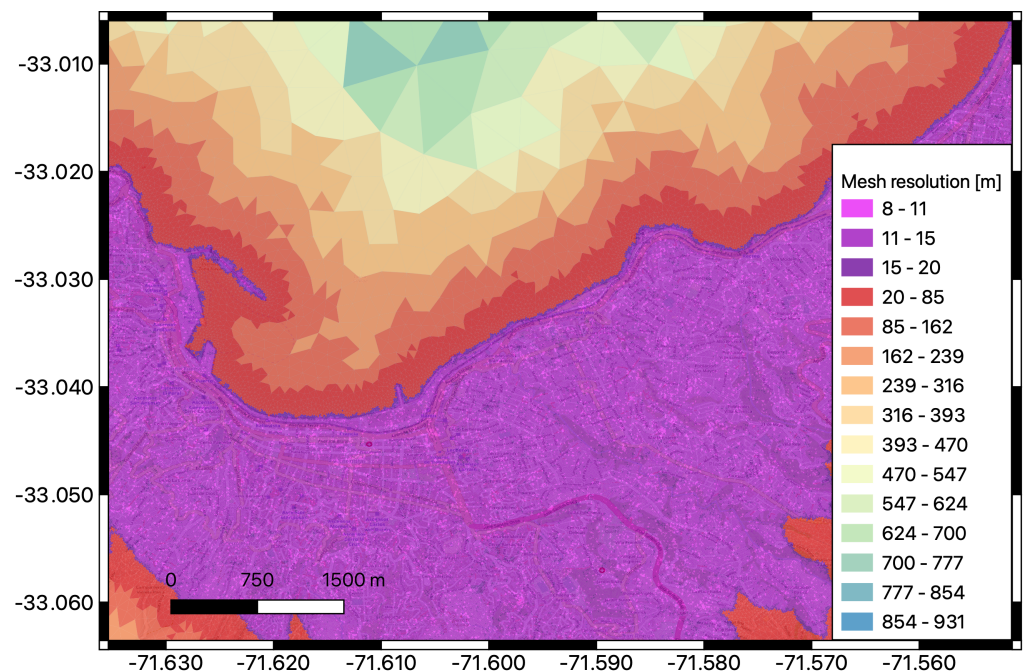


Figure S1. Triangular mesh resolution in a small section of the triangular mesh used in the TsunAWI simulations. The area corresponds to Valparaíso.

Complementary seismic source models: slip distribution

Figure S2 is complementary to the Figure 3 in the main text. Slips models and ground deformation (contours) are shown.

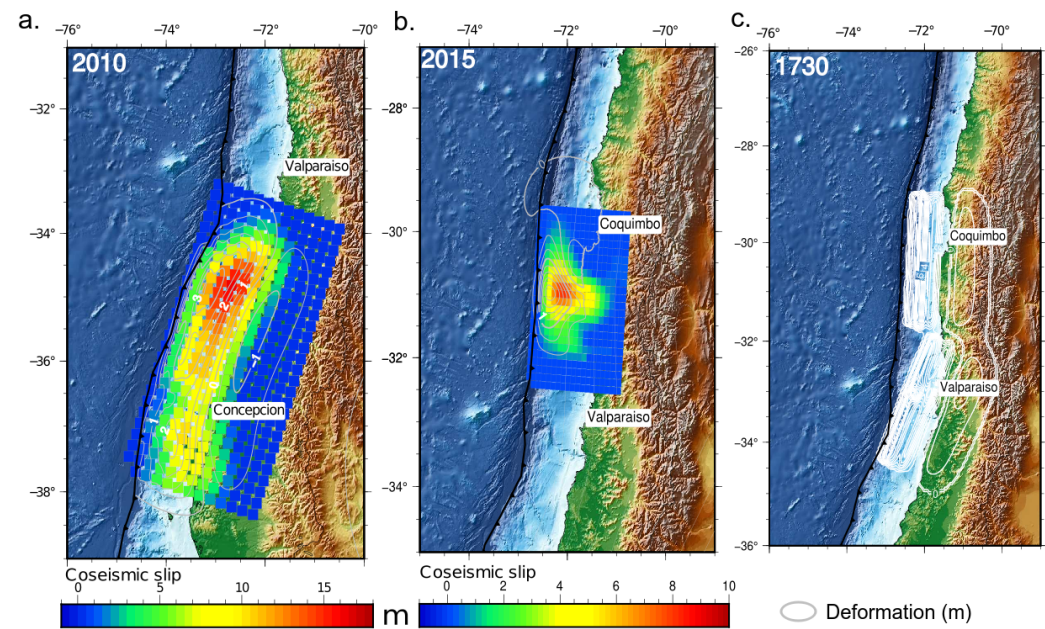


Figure S2. Slip distribution of three cases used in the experiments: a. Maule 2010 Mw 8.8 earthquake [1]; b. Illapel (Coquimbo) Mw 8.3 earthquake [2]; c. Valparaíso Mw 9.1-9.3 earthquake [3]. Basemap: © GEBCO 2019.

Complementary inundation maps based on the Experiment 2015

Figure S3a shows the inundation resulting from Tsunami-HySEA and Figure S3b shows the inundation that resulted with the COMCOT code for the Experiment 2015 in the Coquimbo area. The following figure complements Figure 6 in the main text.

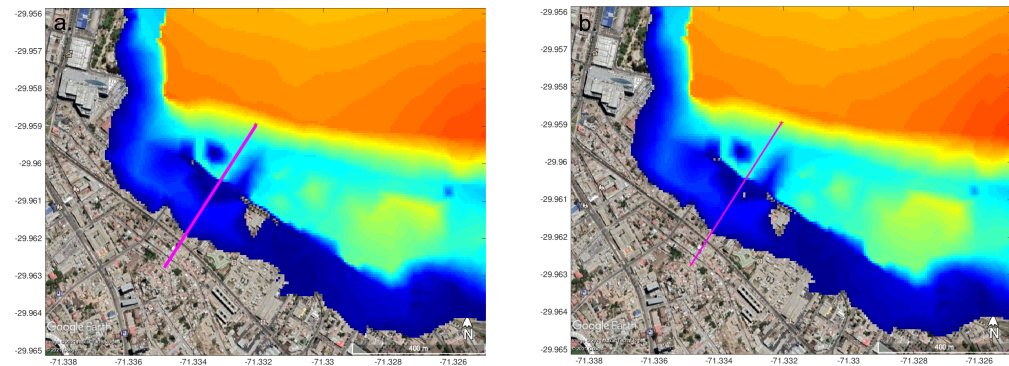


Figure S3. Maximum flow depths along Coquimbo that resulted from two numerical models. a. Maximum flow depth in the inundation areas obtained by the numerical model Tsunami-HySEA for the Manning value of $n=0.025$, for the Experiment 2015. b. Maximum flow depth in the inundation areas obtained by the numerical model COMCOT for the Manning value of $n=0.025$, for the Experiment 2015. Basemap: © Google Earth 2021, Maxar Technologies.

Figure S4 shows regression of inundation area respect to Manning values and different flow depth thresholds (upper panel) based on Experiment 2015 in the Coquimbo area. The inundation area with respect to one Manning value $n=0.025$ is shown in the lower panel.

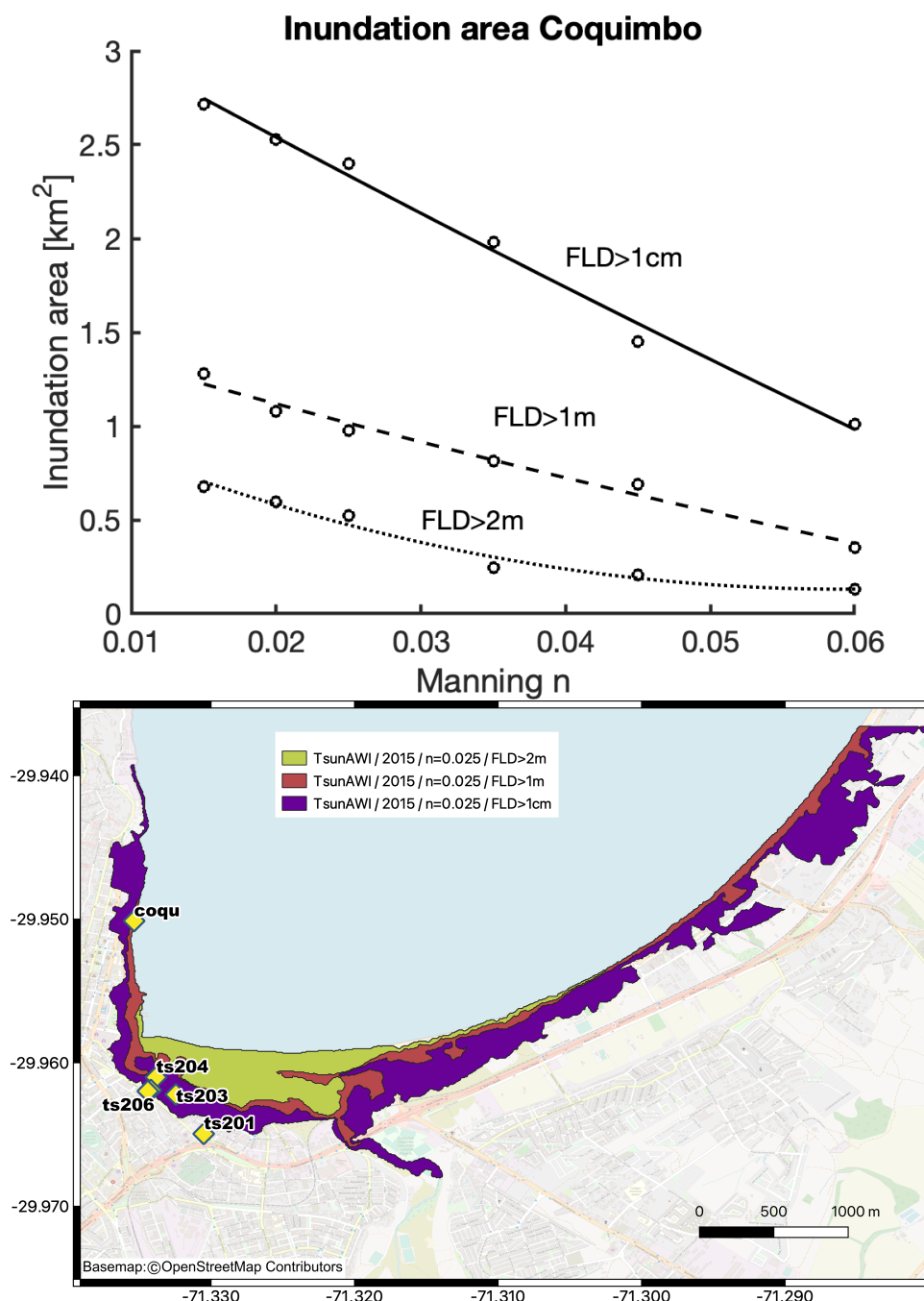


Figure S4. Inundation area along Coquimbo based on the Experiment 2015. Upper panel: Functional relation over the full Manning range. Lower panel: Inundation area for three flow depths thresholds and Manning $n=0.025$ for the Experiment 2015. Basemap: © OpenStreetMap Contributors.

Offshore and inundation of the Experiment 1730

Figure S5a-c shows time series for the DART32402, the selected virtual and real tide gauges for Experiment 1730. Similar analysis is shown in the main text for Experiments 2010 and 2015. Figure S5e summarizes good correlation (except for 3 tide gauges) obtained for this case 1730 for the three numerical codes.

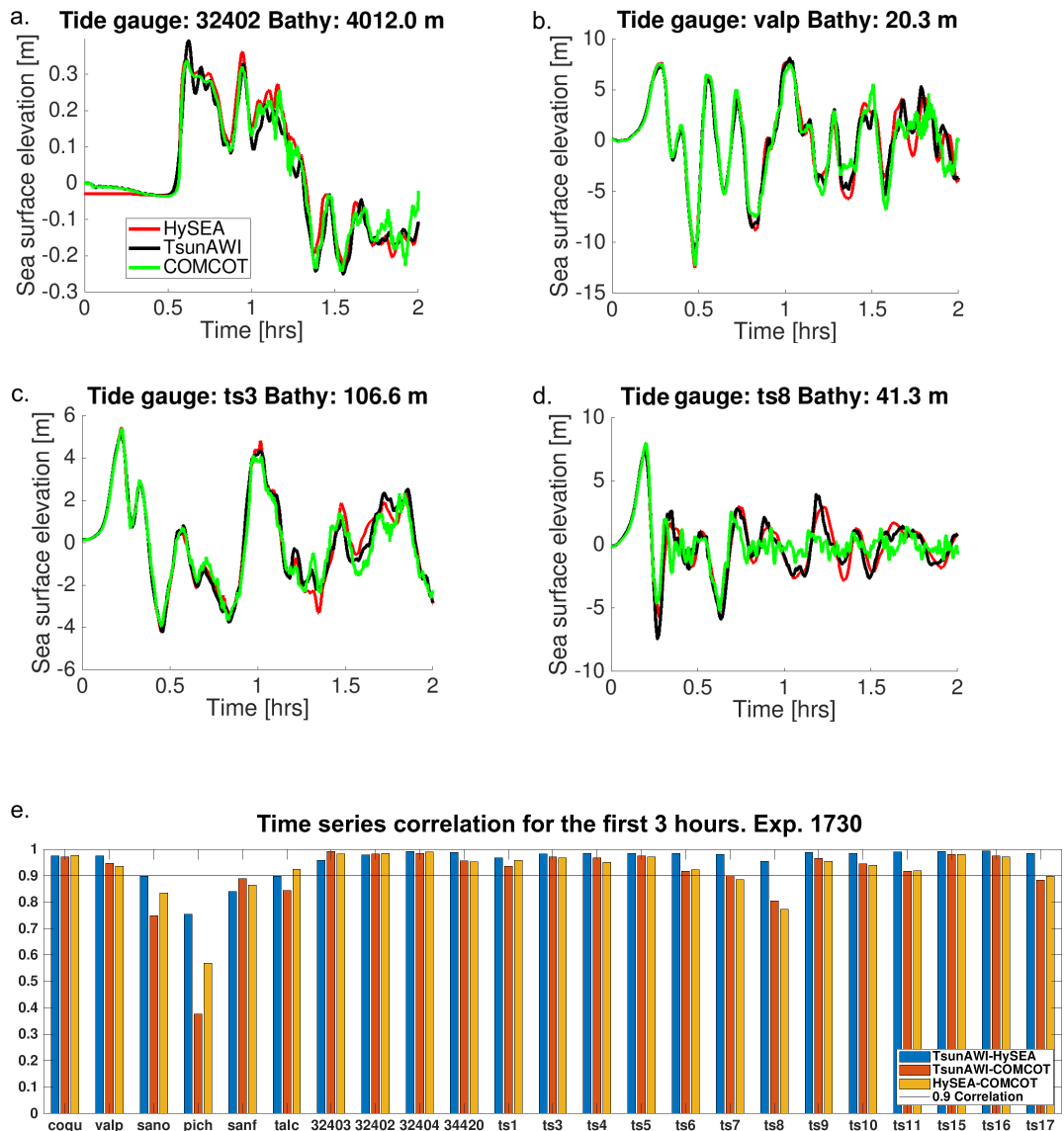


Figure S5. Time series and correlations obtained for all models in the Experiment 1730 in selected locations. Results only shown for Manning $n=0.025$. a. Tide gauge results for the DART 32402. b. Tide series resulted at the 'valp' tide gauge. c. Time series resulted for the 'ts3' tide gauge. d. Time series resulted for the 'ts8' tide gauge. e. Correlations summary for Experiment 1730 based on Manning value of $n=0.025$. The corresponding correlation values are listed in Table 6 in the main text.

Figure S6 shows regression of inundation area with respect to Manning values (upper panel) based on Experiment 1730 along the Coquimbo area. The inundation area with respect to 1cm flow depth threshold and three Manning values is shown in the lower panel. The inundation area shown in Figure S3 (lower panel) is three times larger than the resulted with Experiment 2015 along Coquimbo (refer to Figure 6a in the main text).

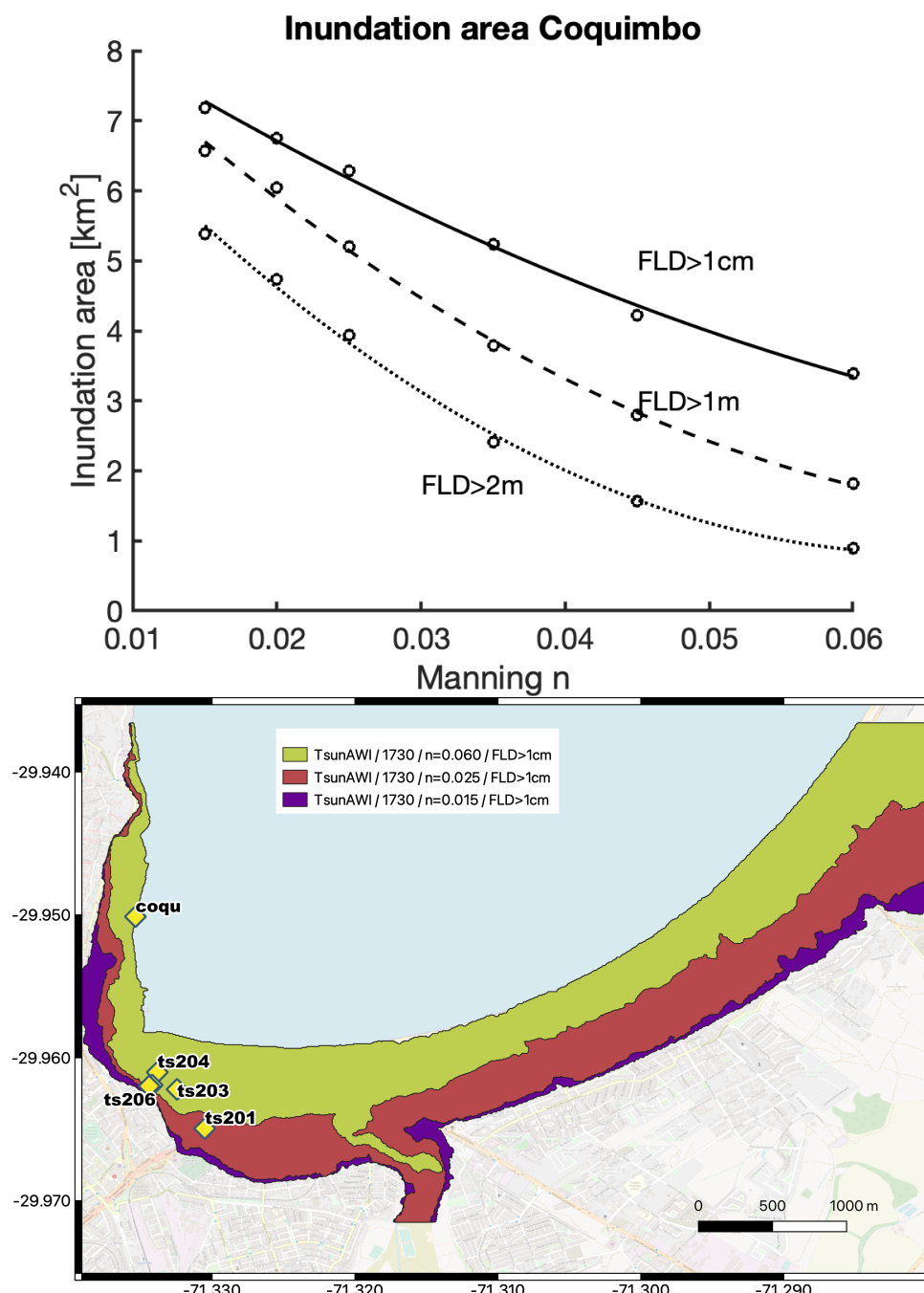


Figure S6. Inundation area along Coquimbo obtained with the TsunAWI code based on experiment 1730. Upper panel: Functional relation over the full Manning range. Lower panel: Inundation area for the three Manning n -values (0.015, 0.025 and 0.060). Basemap: © OpenStreetMap Contributors.

The following tables summarize some properties and statistics of the inundation for Experiment 2015 (Table S1) and Experiment 2017 (Tables S2,S3). These include:

- The location and topography value of the largest runup position (RU_Max, RU_LON, RU_LAT). These positions are shown in Figures 7 and 12 as circles.
- The max. flow depth value and position (Inun_Max, Inun_LON, Inun_LAT). These positions are shown in Figures 7 and 12 as squares.
- Total area of inundation (based on minimum flow depth of 1cm).

- Estimate of the total volume based on the max. flow depth integral over the inundation area.
- mean value and standard deviation of the flow depth in the entire inundation polygon (based on minimum flow depth of 1cm) and a 3hr simulation.
- median, 90th and 75th percentile of the flow depth in the entire inundation polygon (based on minimum flow depth of 1cm) and a 3hr simulation.

All values are given for each model and each Manning value.

Table S1. Summary of statistics of the inundation results for each numerical code based on the Experiment 2015 in Coquimbo. These statistics are based on the maximum inundation point. See Table 5 and Figure 7 in the main text.

TsunAWI code Experiment 2015													
Mn_n	RU_Max	RU_LON	RU_LAT	Inun_Max	Inun_LON	Inun_LAT	Area_km2	Volume_m3	mean	std	prc90	prc75	median
0.015	5.18	-71.32597	-29.96448	5.3	-71.32821	-29.96065	2.714625	4035499	1.37	1.2	3.34	2.18	0.92
0.02	4.68	-71.32934	-29.96476	4.27	-71.3265	-29.95933	2.527271	3312512	1.22	1.1	2.94	2.03	0.78
0.025	4.42	-71.32816	-29.96458	4.13	-71.32174	-29.95926	2.400901	2902456	1.13	1.06	2.76	1.94	0.7
0.035	4.35	-71.32721	-29.96336	3.87	-71.32238	-29.95929	1.980774	2163438	1.03	0.97	2.48	1.72	0.68
0.045	3.58	-71.31922	-29.96023	3.59	-71.32174	-29.95926	1.452577	1567227	1.03	0.9	2.47	1.5	0.83
0.06	3.2	-71.32089	-29.96071	3.15	-71.32266	-29.95926	1.011489	1023315	0.96	0.81	2.29	1.47	0.73
HySEA code Experiment 2015													
0.015	5.01	-71.32595	-29.96429	4.35	-71.32133	-29.95921	2.250956	2946463	1.22	1.06	2.83	2.05	0.83
0.02	4.55	-71.32947	-29.96449	4.24	-71.32153	-29.95921	2.007878	2599730	1.22	1.04	2.75	2.04	0.85
0.025	4.43	-71.32725	-29.96338	4.11	-71.32153	-29.95921	1.735198	2262727	1.22	1.01	2.67	1.99	0.89
0.035	4.19	-71.32732	-29.96331	3.81	-71.32153	-29.95921	1.322512	1673443	1.2	0.93	2.57	1.76	1.07
0.045	3.56	-71.32061	-29.96064	3.48	-71.32211	-29.95921	1.059148	1230767	1.11	0.85	2.47	1.55	0.99
0.06	3.07	-71.32227	-29.96077	2.99	-71.32211	-29.95921	0.769024	785086.3	0.99	0.77	2.23	1.55	0.7
COMCOT code Experiment 2015													
0.015	4.97	-71.32736	-29.96559	4.47	-71.32132	-29.95921	2.503374	3362771	1.25	1.06	2.9	1.98	0.85
0.02	4.59	-71.32938	-29.96461	4.34	-71.32132	-29.95921	2.270397	2949062	1.22	1.04	2.8	1.97	0.83
0.025	4.43	-71.32724	-29.96338	4.18	-71.32132	-29.95921	1.986203	2532071	1.19	1.01	2.67	1.93	0.87
0.035	4.13	-71.3273	-29.96325	3.84	-71.32208	-29.95921	1.490075	1816887	1.17	0.93	2.58	1.7	0.99
0.045	3.64	-71.3219	-29.96084	3.51	-71.32254	-29.95921	1.124089	1300861	1.11	0.84	2.47	1.52	0.96
0.06	3.03	-71.32071	-29.96064	2.96	-71.32254	-29.95921	0.819789	788493.7	0.95	0.77	2.2	1.51	0.65

Table S2. Summary of statistics of the inundation results for each numerical code based on the Experiment 1730 in Viña del Mar. These statistics are based on the maximum inundation area for each Manning n -values. See Table 7, Figure 9e,f and Figure 11 in the main text. *: These values are considered outliers after 3 hours of simulation.

TsunAWI code Experiment 1730 in Viña del Mar													
Mn_n	RU_Max	RU_LON	RU_LAT	Inun_Max	Inun_LON	Inun_LAT	Area_km2	Volume_m3	mean	std	prc90	prc75	median
0.015	11.77	-71.52406	-33.03666	10.32	-71.55117	-33.00548	5.396223	19628820	3.1	1.87	5.51	4.12	2.94
0.02	11.13	-71.54812	-33.00527	10.27	-71.5518	-33.00708	4.913805	18060780	3.14	1.81	5.43	4.45	3.01
0.025	11.13	-71.54812	-33.00527	10.28	-71.5518	-33.00708	4.760982	16865070	3.03	1.81	5.29	4.36	2.93
0.035	11.13	-71.54812	-33.00527	10.27	-71.5518	-33.00708	4.473159	14745250	2.82	1.84	5.12	4.18	2.69
0.045	10.94	-71.54842	-33.00555	10.26	-71.5518	-33.00708	3.945906	13190960	2.87	1.78	5.16	4.12	2.72
0.06	10.17	-71.54793	-33.0051	10.19	-71.5518	-33.00708	3.791677	11558530	2.67	1.83	5.1	3.89	2.45
HySEA code Experiment 1730 in Viña del Mar													
0.015	13.05	-71.54633	-33.00329	11.39	-71.57556	-33.02685	4.899994	16728660	2.94	1.72	5.09	4.14	2.71
0.02	12.4	-71.54685	-33.00491	11.26	-71.55063	-33.00361	4.713264	15752070	2.88	1.75	5.05	4.17	2.7
0.025	12.4	-71.54685	-33.00491	11.15	-71.5505	-33.00296	4.528798	14953210	2.84	1.79	5.01	4.17	2.67
0.035	12.4	-71.54685	-33.00491	11.18	-71.5505	-33.00296	3.973825	13647810	2.97	1.76	5.2	4.2	2.83
0.045	12.4	-71.54685	-33.00491	11.19	-71.5505	-33.00296	3.686674	12565260	2.95	1.81	5.33	4.19	2.78
0.06	12.4	-71.54685	-33.00491	11.22	-71.5505	-33.00296	3.355377	11329340	2.93	1.88	5.42	4.24	2.71
COMCOT code Experiment 1730 in Viña del Mar													
0.015	11.65	-71.54932	-33.00413	11.13	-71.55075	-33.00322	4.799514	16358360	2.93	1.71	5.04	4.12	2.69
0.02	38.44*	-71.54541	-33.00316	18.55	-71.55069	-33.00316	4.741771	16464600	3.01	1.95	5.14	4.21	2.77
0.025	11.65	-71.54932	-33.00413	11.13	-71.55075	-33.00322	4.449616	14624990	2.83	1.79	4.96	4.09	2.66
0.035	23.04*	-71.54706	-33.00329	16.61	-71.57568	-33.02666	3.929966	13653830	3.01	1.87	5.28	4.16	2.83
0.045	11.65	-71.54932	-33.00413	11.08	-71.55075	-33.00322	3.590738	12025300	2.9	1.82	5.28	4.07	2.69
0.06	11.55	-71.54913	-33.00387	11.01	-71.55075	-33.00322	3.087109	10630310	2.85	1.89	5.35	4.1	2.58

Table S3. Summary of statistics of the inundation results for each numerical code based on the Experiment 1730 in Valparaíso. These statistics are based on the maximum inundation area for each Manning n -values. See Table 7 and Figures 9c,d in the main text. *: These values are considered outliers after 3 hours of simulation.

TsunAWI code Experiment 1730 Valparaíso													
Mn_n	RU_Max	RU_LON	RU_LAT	Inun_Max	Inun_LON	Inun_LAT	Area_km2	Volume_m3	mean	std	prc90	prc75	median
0.015	12.07	-71.63044	-33.03978	10.5	-71.62759	-33.03467	2.387829	10573360	3.89	1.94	6.17	5.24	4.23
0.02	11.04	-71.63123	-33.03426	10.29	-71.62718	-33.03149	2.320221	9387629	3.56	1.81	5.62	4.77	3.83
0.025	10.82	-71.63129	-33.03406	10.3	-71.62718	-33.03149	2.179979	8422709	3.41	1.6	5.26	4.42	3.6
0.035	9.87	-71.63134	-33.03711	10.31	-71.62718	-33.03149	2.044707	6832824	2.97	1.35	4.36	3.72	3.1
0.045	9.01	-71.63104	-33.03401	10.28	-71.62718	-33.03149	1.952494	5643106	2.59	1.23	3.64	3.13	2.63
0.06	8.17	-71.58908	-33.03199	9.95	-71.62718	-33.03149	1.871035	4609247	2.23	1.19	3.3	2.54	2.23
HySEA code Experiment 1730 Valparaíso													
0.015	10.6	-71.58845	-33.03467	9.09	-71.61293	-33.04294	2.138855	7798866	3.25	1.4	4.61	3.97	3.5
0.02	10.59	-71.5891	-33.03447	9.02	-71.59047	-33.03115	2.096974	7316309	3.11	1.33	4.49	3.79	3.25
0.025	10.25	-71.58839	-33.03363	9.02	-71.59047	-33.03115	2.058844	6846122	2.97	1.28	4.32	3.61	3.05
0.035	10	-71.58897	-33.03447	9.02	-71.59047	-33.03115	2.000516	6248156	2.8	1.2	3.98	3.34	2.87
0.045	9.78	-71.58858	-33.03395	9.01	-71.58969	-33.03076	1.956125	5921528	2.72	1.18	3.76	3.21	2.77
0.06	9.53	-71.58878	-33.03265	9	-71.58969	-33.03076	1.902899	5541367	2.63	1.18	3.54	3.07	2.72
COMCOT code Experiment 1730 Valparaíso													
0.015	10.38	-71.58844	-33.03356	9.01	-71.58969	-33.03076	2.089562	6938136	2.97	1.31	4.28	3.61	3.02
0.02	10.12	-71.58832	-33.03382	9	-71.58969	-33.03076	2.069889	6884230	2.98	1.33	4.35	3.64	3
0.025	10.08	-71.5885	-33.03356	9	-71.58969	-33.03076	2.035679	6526571	2.88	1.28	4.1	3.48	2.9
0.035	16.45*	-71.63202	-33.02685	14.75	-71.63141	-33.02634	2.084515	8348013	3.6	2.13	6.19	4.91	3.14
0.045	9.56	-71.5889	-33.03278	8.95	-71.58969	-33.03076	1.936292	5657249	2.63	1.18	3.62	3.05	2.68
0.06	9.42	-71.58884	-33.03265	8.89	-71.58969	-33.03076	1.876439	5189862	2.51	1.17	3.39	2.9	2.56

References

- Moreno, M.; Rosenau, M.; Oncken, O. 2010 Maule earthquake slip correlates with pre-seismic locking of Andean subduction zone. *Nature* **2010**, *467*, 198–202. doi:10.1038/nature09349.
- Shrivastava, M.N.; González, G.; Moreno, M.; Chlieh, M.; Salazar, P.; Reddy, C.D.; Báez, J.C.; Yáñez, G.; González, J.; de la Llera, J.C. Coseismic slip and afterslip of the 2015 Mw 8.3 Illapel (Chile) earthquake determined from continuous GPS data. *Geophysical Research Letters* **2016**, *43*, 10,710–10,719, [https://agupubs.onlinelibrary.wiley.com/doi/pdf/10.1002/2016GL070684]. doi:https://doi.org/10.1002/2016GL070684.
- Carvajal, M.; Cisternas, M.; Catalán, P. Source of the 1730 Chilean earthquake from historical records: Implications for the future tsunami hazard on the coast of Metropolitan Chile. *Journal of Geophysical Research: Solid Earth* **2017**, *122*, 3648–3660.